Characterization of Abnormal Optic Nerve Head Morphology in Albinism Using Optical Coherence Tomography

Sarim Mohammad, Irene Gottlob, Viral Sheth, Anastasia Pilat, Helena Lee, Ellen Pollheimer, and Frank Anthony Proudlock

University of Leicester Ulverscroft Eye Unit, University of Leicester, Faculty of Medicine and Biological Sciences, Robert Kilpatrick Clinical Sciences Building, Leicester Royal Infirmary, Leicester, United Kingdom

Correspondence: Frank Anthony Proudlock, University of Leicester Ulverscroft Eye Unit, University of Leicester, Faculty of Medicine and Biological Sciences, Robert Kilpatrick Clinical Sciences Building, Leicester Royal Infirmary, PO Box 65, Leicester, LE2 7LX, UK; fap1@le.ac.uk.

SM and IG are joint first authors.

Submitted: March 12, 2015
Accepted: May 19, 2015

Citation: Mohammad S, Gottlob I, Sheth V, et al. Characterization of abnormal optic nerve head morphology in albinism using optical coherence tomography. *Invest Ophthalmol Vis Sci*. 2015;56:4611–4618. DOI:10.1167/iovs.15-16856

Purpose. To characterize abnormalities in three-dimensional optic nerve head (ONH) morphology in people with albinism (PWA) using spectral-domain optical coherence tomography (SD-OCT) and to determine whether ONH abnormalities relate to other retinal and clinical abnormalities.

Methods. Spectral-domain OCT was used to obtain three-dimensional images from 56 PWA and 60 age- and sex-matched control subjects. B-scans were corrected for nystagmus-associated motion artefacts. Disc, cup, and rim ONH dimensions and peripapillary retinal nerve fiber layer (ppRNFL) thickness were calculated using Copernicus and ImageJ software.

Results. Median disc areas were similar in PWA (median = 1.65 mm^2) and controls (1.71 mm^2, $P = 0.128$), although discs were significantly elongated horizontally in PWA ($P < 0.001$). In contrast, median optic cup area in PWA (0.088 mm^2) was 23.7% of that in controls (0.373 mm^2, $P < 0.001$), with 39.4% of eyes in PWA not demonstrating a measurable optic cup. This led to significantly smaller cup to disc ratios in PWA ($P < 0.001$). Median rim volume in PWA (0.273 mm^3) was 136.6% of that in controls (0.200 mm^3). The ppRNFL was significantly thinner in PWA compared with controls ($P < 0.001$), especially in the temporal quadrant. In PWA, ppRNFL thickness was correlated to ganglion cell thickness at the central fovea ($P = 0.007$). Several ONH abnormalities, such as cup to disc ratio, were related to higher refractive errors in PWA.

Conclusions. In PWA, ocular maldevelopment is not just limited to the retina but also involves the ONH. Reduced ppRNFL thickness is consistent with previous reports of reduced ganglion cell numbers in PWA. The thicker rim volumes may be a result of incomplete maturation of the ONH.

Keywords: albinism, optical coherence tomography, optic nerve head

Albinism is a group of congenital disorders in melanin biosynthesis affecting approximately 1 in 4000 people.[1] Albinism leads to a range of visual system abnormalities, including iris transillumination and thinning,[2] high refractive errors,[3,4] foveal hypoplasia,[5] failure of photoreceptor specialization,[5] absence of the foveal avascular zone and rod-free area,[6] and misrouting of the optic nerve at the chiasm due to greater contralateral crossing of axons.[7] These visual system abnormalities can coexist with either the absence or presence of pigmentation disorders of the hair and skin, leading to a differentiation between ocular albinism (OA) and oculocutaneous albinism (OCA), respectively.

Although chiasmal abnormalities are well documented, little is known about the morphology of the optic nerve head (ONH) in albinism. Using fundus photography, Spedick and Beauchamp[8] reported typical optic nerve hypoplasia in 6 eyes of 12 people with albinism (PWA), and subtle optic nerve hypoplasia in an additional 10 eyes. With magnetic resonance imaging, Schmitz et al.[9] also found smaller postorbital optic nerves compared with controls in 17 PWA. Tilted discs also have been described in albinism.[10]

Spectral domain-optical coherence tomography (SD-OCT) is a high-resolution three-dimensional ocular imaging technique. We recently used SD-OCT to characterize iris[2] and the foveal[5,11] abnormalities in albinism. Only one group has so far described the ONH in albinism using SD-OCT. Chong et al.[12] observed an elevation of the optic nerve in four of six PWA using SD-OCT, although the ONH was not described in detail.

The aim of the present study was to use SD-OCT to characterize ONH morphology in albinism using a sample representative of the spectrum of abnormalities. Misalignment of B-scans caused by nystagmus leads to difficulties in analyzing volumetric scans in albinism. We have used the retinal vasculature and optic disc margins on fundus photography to realign B-scans, which is possible because the nystagmus is invariably horizontal.[13] To investigate ONH structure in albinism our specific aims were to characterize ONH topography (i.e., disc, rim, and cup dimensions) compared with controls, analyze peripapillary retinal nerve fiber layer

(ppRNFL) thickness since mis-wiring of retinal projections is known to occur in PWA,[14] compare ONH and ppRNFL abnormalities with foveal abnormalities, and compare ONH and ppRNFL abnormalities with other clinical measures, such as refractive error, best-corrected visual acuity, and asymmetry of VEPs.

Methods

Patients

Thirty-three male and 23 female PWA (median age = 34 years, range, 17–62 years) were recruited to the study from pediatric and adult neuro-ophthalmology clinics at the Leicester Royal Infirmary. Before inclusion, the nature and consequences of the study were explained and informed consent was obtained. The study was conducted in keeping with the Declaration of Helsinki and was approved by local research and ethics committees.

Diagnosis of albinism was based on the presence of three signs: VEP asymmetry, foveal hypoplasia on a macular OCT scan, and iris transillumination. Visual evoked potential testing was carried out in accordance with International Society for Clinical Electrophysiology of Vision standards. Although not an inclusion criterion, all the patients demonstrated some degree of horizontal nystagmus. Fundi were examined for tilted discs clinically and using fundus photography.[15,16]

Sixty healthy control volunteers with no known ophthalmic or neurological disease were also recruited from within the University of Leicester and Leicester Royal Infirmary, including healthy spouses of patients and members of staff (36 male, 24 female volunteers; median age = 35 years, range, 18–63 years). Control volunteers were excluded if they had significant refractive error (spherical equivalent ≥ 3 or ≤ -3 diopters).

Scan Acquisition

A high-resolution SD-OCT device with a rapid acquisition rate (axial resolution = 3 μm, 52,000 = A scans/s; SOCT Copernicus HR; OPTOPOL Technology S.A., Zawiercie, Poland) was used to obtain volumetric ONH and foveal images in both eyes ($7 \times 7 \times 2$ mm, 75 B-scans, 750 A-scans/B-scan). The acquisition time for each B-scan was 14.4 ms, minimizing motion artifact caused by nystagmus. Macular SD-OCT scans were acquired and analyzed in accordance with previously published methodology.[5]

Image Analysis

B-Scan Realignment. The B-scans were realigned on all participants with albinism (because all had nystagmus) by comparing SD-OCT scans with the contours of retinal vessels and disc margins from fundus photographs. A custom written macro in ImageJ (http://imagej.nih.gov/ij/; provided in the public domain by the National Institutes of Health, Bethesda, MD, USA) was used to realign B-scans (see Supplementary Fig. S1).

Optic Nerve Head Morphology. Cup, disc, and rim dimensions were calculated using SOCT Copernicus Software. The software automatically detects the internal limiting membrane (ILM) and the RPE borders, which were used to define disc margins. Cup and rim dimensions were determined using a plane anteriorly offset 150 μm parallel to the disc plane (see Supplementary Fig. S2). Within the disc margins, absence of tissue posterior to the offset is designated as cup and presence of tissue anterior to the offset as rim. Measurements in the retinal plane were adjusted using refractive error following manufacturer's instructions based on measurements with artificial eyes with extended or reduced axial lengths (correction factor = –0.0175*spherical equivalent + 0.965). To determine the angle of major axis of the disc in en face view, ImageJ software was used to fit an ellipse to the disc edges on the fundus image (for an example see Supplementary Fig. S3). The angle was calculated where ovality was greater than 10% (i.e., where the ratio of the length of the longer axis/shorter axis > 1.1).

Nasal and Temporal Rim. A cross-sectional analysis of the ONH along the naso-temporal axis was performed from a single horizontal B-scan where the cup was at its deepest using an ImageJ macro to analyze temporal and nasal rim width, peak height, height at edge of the disc, and cup and rim area (parameters not provided by the automated Copernicus SD-OCT software). The macro incorporated the ABSnake plug-in (http://imagejdocu.tudor.lu/doku.php?id=plugin:segmentation:active_contour:start) to detect the ILM.

Peripapillary RNFL Thickness. The ppRNFL was estimated using the automated algorithm in the Copernicus SD-OCT software that automatically detects the ppRNFL edges and disc margins, which were manually checked and adjusted. The ppRNFL thickness was measured in two annuli: 1.6 to 2.4 mm diameter, and 2.4 to 3.2 mm diameter each divided into 10 radial segments (using the GDx Nerve Fiber Analyzer protocol, Carl Zeiss Meditec). Analysis of ppRNFL was not possible on 4 of the 56 participants mainly due to large nystagmus widening the extent of shadows caused by the iris.

Reliability of Measures. Test–retest of ONH and ppRNFL parameters, performed by repeating the analysis on two separate SD-OCT scans (PWA: $n = 37$; controls: $n = 27$), demonstrated high repeatability (intraclass correlation coefficients > 0.9 for all parameters, see Supplementary Table S1).

Statistical Analysis

We used SPSS software version 16.0 (SPSS, Inc., Chicago, IL, USA) to carry out statistical analyses. Due to nonnormality of the data, ONH and ppRNFL parameters were compared between albinism and controls using Mann-Whitney tests after averaging right and left eyes. Linear mixed models were used to determine the relationship between ONH parameters and (1) retinal layers at the fovea (see Ref. 5 for analysis), including macular thickness (MT, from ILM to Bruch's membrane [BM]), inner layers (from ILM to the posterior border of the outer plexiform layer [OPL], i.e., layers mostly absent in the normal retina continuing over the fovea in albinism), outer layers (from the posterior border of the OPL to the BM, i.e., layers related to the photoreceptors and retinal pigment epithelium), and ganglion cell layer (GCL); (2) clinical measures, that is, best-corrected visual acuity, refractive error (spherical equivalent, including each eye separately in the model) and VEP asymmetry; and (3) age, sex, and eye.

Results

Clinical Features of Albinism Cohort

The clinical features of the albinism cohort are shown in Supplementary Table S2.[17] All of the OA phenotype were male, whereas similar proportions of males and females were observed in the OCA phenotype. Best-corrected visual acuities ranged from 0.18 to 1.1 logMAR. As previously reported,[3,4] significant refractive errors existed in the albinism group with high levels of hyperopia and with-the-rule astigmatism (in 89.5% of the 23.4% of the PWA who had significant astigmatism [cylinder $\geq +3$D or ≤ -3D]). High proportions of strabismus and anomalous head posture were encountered. All PWA

showed foveal hypoplasia of varying degrees and horizontal nystagmus.

Optic Nerve Head Morphology

The spectrum of ONH abnormalities is represented in Supplementary Figure S3, comparing fundus photography with SD-OCT. On examination of B-scans, a large number of PWA had enlarged nasal rims and small or nonexistent cups compared with controls (see example shown in Supplementary Fig. S4). On analyzing ONH scans using SD-OCT, 39.4% of eyes in the albinism group did not have a measurable optic cup (i.e., the base of the cup did not reach 150 μm anterior to the disc plane), whereas all the control eyes displayed a cup.

En Face View. Analysis of the optic disc, cup, and rim areas in en face view are illustrated schematically in Figure 1. Disc areas were similar in PWA and controls (medians = 1.65 mm^2 and 1.71 mm^2, respectively, $P = 0.128$), although disc areas were more narrowly distributed in the control group. Median cup area was significantly smaller in PWA compared with controls (0.088 mm^2 and 0.373 mm^2, respectively, $P < 0.001$), although some cup areas in PWA were within normal ranges. Not surprisingly, cup to disc area ratios were much smaller in PWA compared with controls (0.059 and 0.267, respectively, $P < 0.001$). Rim areas (i.e., disc area–cup area) were slightly larger in PWA compared with controls (1.42 mm^2 and 1.25 mm^2, respectively, $P = 0.04$).

The angle of the disc in en face view was calculated in 53.8% of PWA and 39.4% of controls (i.e., where ovality of the optic disc > 10%). In albinism, the most common orientation was near the horizontal axis or rotated slightly with the nasal disc more superior to the temporal disc (see Supplementary Fig. S5). In contrast, in the control group, discs were more commonly oriented along or near the vertical axis. Relative horizontal elongation of optic discs in albinism was also apparent from the distribution of horizontal/vertical disc ratios (more frequently >1 in albinism compared with controls, see Figs. 1E, 1J).

On clinical examination of fundi and fundus images, two PWA displayed signs of tilted disc syndrome (with an inferior or inferonasal crescent of visible sclera and inferonasal disc tilt)[15] and one PWA myopic tilted disc pattern (with temporal crescent of visible sclera, temporal disc torsion, and significant myopia).[16]

Cross-Sectional View. Figure 2 shows a schematic cross-sectional view of the optic discs along the naso-temporal axis. Both nasal and temporal rim areas were significantly larger in the albinism group (medians: 0.176 mm^2 and 0.038 mm^2, respectively) compared with controls (0.101 mm^2 and 0.015 mm^2, respectively; $P < 0.001$). The asymmetry of temporal and nasal rim areas (i.e., nasal rim area/nasal + temporal rim areas) was not significantly different between the two groups (median = 0.83 in albinism, 0.86 in controls; $P = 0.144$).

Median cup volumes, estimated from all B-scans spanning the ONH, were much smaller in PWA compared with controls (median = 0.009 mm^3 and 0.068 mm^3, respectively; $P < 0.001$, Figs. 2B, 2E). Rim volumes were significantly larger in PWA compared with controls (medians = 0.273 mm^3 and 0.200 mm^3, respectively; $P = 0.036$, Figs. 2C, 2F).

Peripapillary RNFL

Figure 3 summarizes the differences in ppRNFL between the albinism and control groups in 10 segments around the ONH (using the GDx Nerve Fiber Analyzer protocol, Carl Zeiss Meditec). Blue colors indicate that the overall ppRNFL thickness in the outer annulus (2.4–3.2 mm) was consistently thinner in albinism ($P \ll 0.0001$). However, these differences were greater in the temporal retina. Overall ppRNFL thickness in the inner annulus (1.6–2.4 mm) was much closer to control values (comparison of overall thickness was $P = 0.89$). However, the nasal aspect was significantly thicker in albinism compared with controls and the temporal aspect significantly thinner ($P < 0.01$).

Consistency of Left and Right Eyes

Intrasubject variation between right and left eyes was relatively small in both the albinism and control groups for ONH parameters (interclass correlation coefficients; PWA: disc area = 0.91, cup area = 0.93, rim area = 0.92, cup volume = 0.90, rim volume = 0.92; controls: disc area = 0.83, cup area = 0.83, rim area = 0.87, cup volume = 0.83, rim volume = 0.89). Intrasubject variation between right and left eyes for ppRNFL was less in PWA (inner ring = 0.91, outer ring = 0.95) compared with controls (inner ring = 0.78, outer ring = 0.75). Interestingly, ppRNFL was significantly thicker in right eyes of PWA compared with left eyes for the outer annulus ($P = 0.001$). This was not related to eye dominance ($P = 0.32$).

Relationship Between Disc/ppRRNFL Abnormalities and Foveal Abnormalities

There were no significant correlations between ONH parameters and central foveal layers in PWA (Table 1). However, GCL thickness at the central fovea and mean ppRNFL thickness in the outer annulus were strongly correlated. Further analysis of nasal and temporal aspects of the ppRNFL (nasal ppRNFL: average of segments 7–10; temporal ppRNFL: segments 2–5) showed a significant correlation between the central foveal GCL thickness and nasal ppRNFL in both inner ($P = 0.016$, $r = 0.374$) and outer annuli ($P = 0.035$, $r = 0.353$) but not with temporal ppRNFL.

Relationship Between Disc/ppRNFL Abnormalities and Clinical Measures

Refractive error was negatively correlated to disc and cup area, and cup to disc ratio and positively correlated to inner ppRNFL (Table 2). Best-corrected visual acuity was also negatively correlated to disc size. The VEP asymmetry was not correlated to any ONH parameter.

Neither age, sex, nor eye measured had any significant influence on optic nerve areas (disc, cup, rim), volumes (rim and cup), cup to disc and horizontal to vertical disc ratios, or inner or outer ppRNFL in either PWA or controls ($P > 0.05$), with the exception of outer ppRNFL, which was thicker in the right eye of PWA as mentioned earlier.

There were no statistically significant differences between OCA and OA groups for any ONH or ppRNFL parameter ($P > 0.05$ for all comparisons).

Discussion

Optic Nerve Head Morphology

In this study we have used high-resolution SD-OCT to systematically characterize three-dimensional ONH topography in albinism, revealing similar-sized optic discs in albinism compared with controls but abnormally smaller or absent optic cups and significantly larger rim volumes. These findings confirm the observation by Chong et al.[12] that the ONH in albinism "appeared very prominently elevated" (i.e., that rims are enlarged). However, the findings are in contrast with the

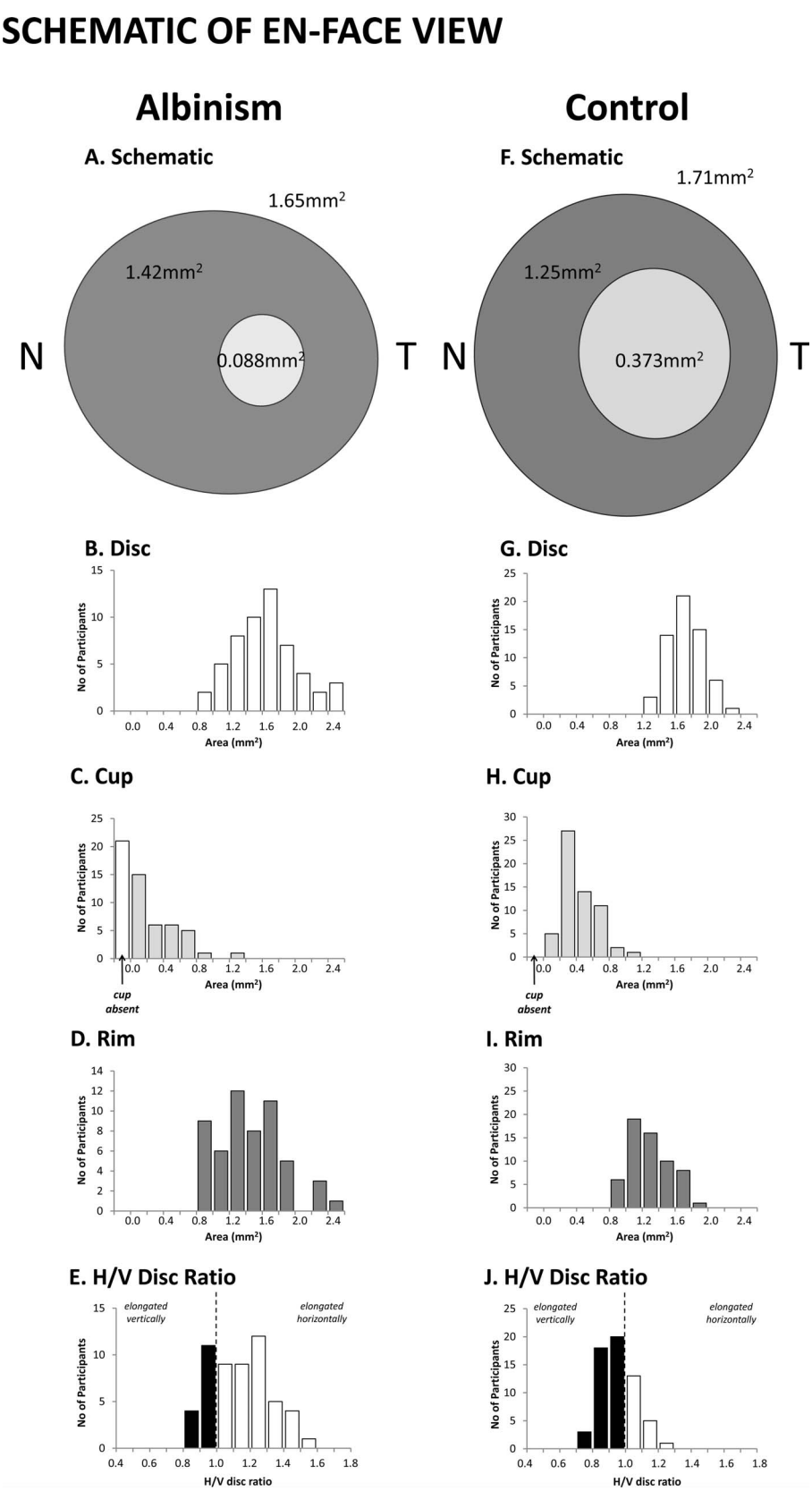

FIGURE 1. Schematic figures of median ONH dimensions in en face view with the distributions of values shown below. (**A**, **F**) Schematic diagrams representing the median dimensions (of both eyes) of participants with albinism and controls for disc, rim, and cup in en face view. The outer ellipse represents the disc area, the inner ellipse the cup area (*light gray*). The *dark gray* color represents the rim area. Distributions of disc, cup, rim areas, and cup to disc ratio (for area measures) for each group are shown in (**B**–**E**) for albinism and (**G**–**J**) for controls, respectively.

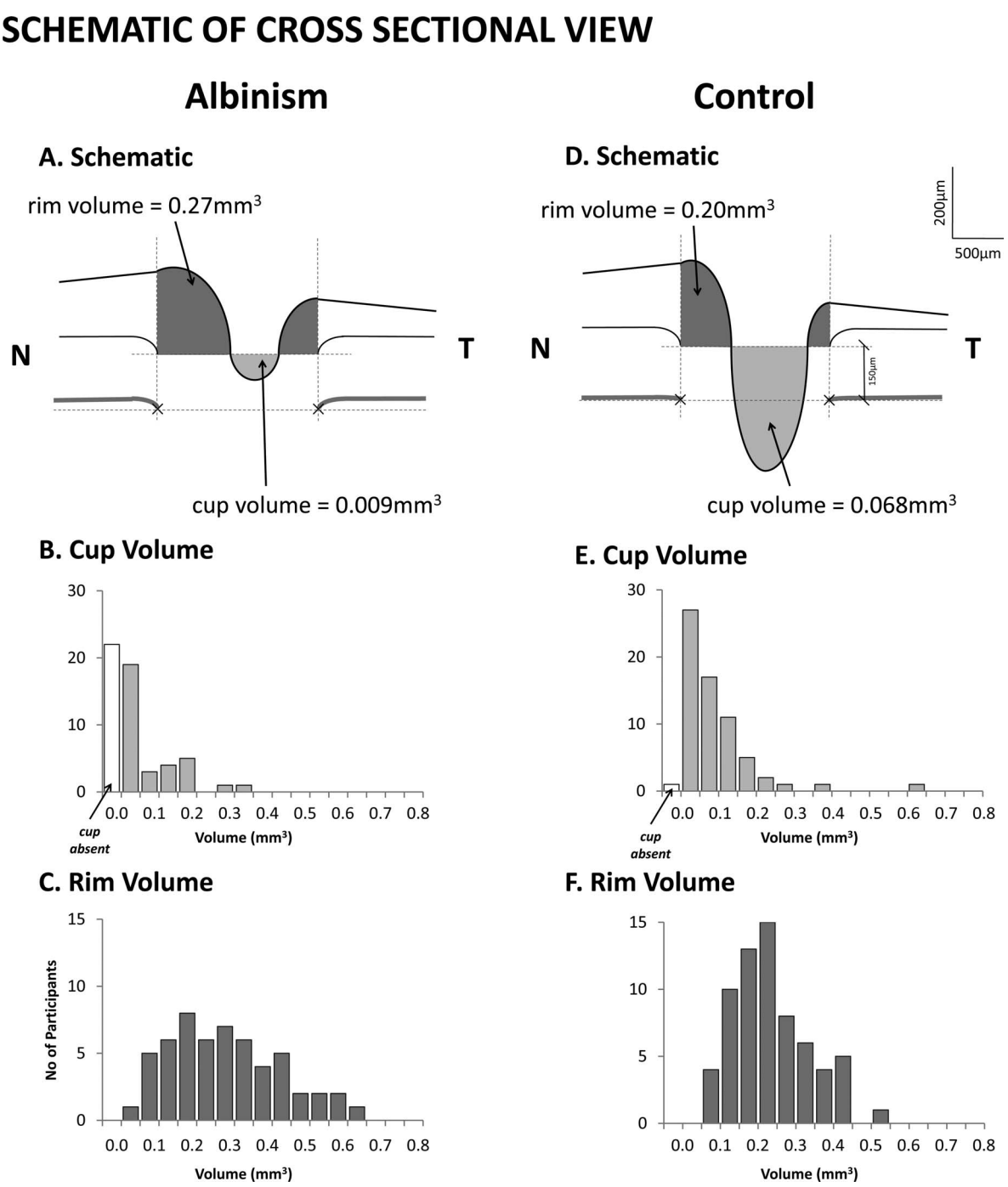

FIGURE 2. Schematic figures of median optic nerve head dimensions in cross-sectional view with the distributions of values. (**A**) Albinism. (**D**) Controls. The *horizontal dotted lines* represent the plane used for the measurement of the disc, rim, and cup areas displayed in Figure 1. This plane, along with the disc edges (defined by the limits of the RPE indicated by the *vertical dotted lines*) and the ILM, was used to calculate cup and rim volumes the distributions of which are shown in (**B**, **C**) for the albinism group and (**E**, **F**) for controls, respectively. N, nasal; T, temporal.

findings of Spedick and Beauchamp,[8] who described hypoplastic nerves seen on fundus photography.

Despite similar-sized optic discs in albinism and controls, the shape of the discs in the two groups was different. Horizontal elongation of discs was commonly observed in albinism where the most common orientation of the disc (where ovality > 10%) was along or near the horizontal axis. In the control group, discs were more commonly oriented along or near the vertical axis. Horizontal elongation of discs is frequently seen in tilted disc syndrome.[15] However, ppRNFL thinning was more significant in the temporal quadrant in albinism, which does not match the pattern of nasal and superior quadrant thinning observed in tilted disc syndrome. Hyperopia was more common than myopia in our albinism study sample, suggesting that myopic tilted discs[16] were not the underlying cause of disc abnormalities.

It is well known that the zone of transition of fibers projecting ipsilaterally and contralaterally is temporally dis-

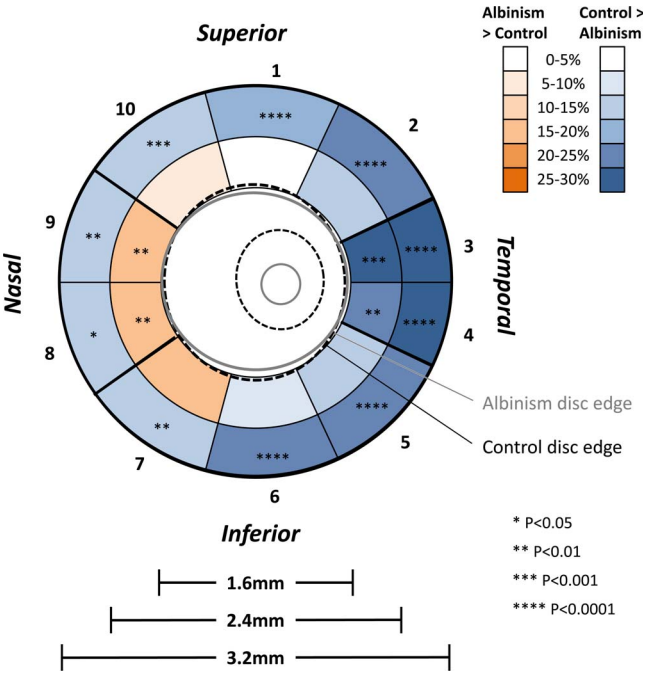

FIGURE 3. Percentage difference in mean ppRNFL thickness between participants with albinism and controls. The *blue* colors indicate ppRNFL is thinner in albinism compared with controls and *red* colors indicate ppRNFL is thicker in albinism compared with controls. The *gray ellipse* indicates the median disc and cup edges in albinism and the *black dashed line* in controls.

placed away from the midline of the retina in albinism.[14] One possibility is that the abnormal distribution of retinal nerve fibers approaching the ONH in albinism led to abnormally shaped discs. Differences we observed in the reorganization of the inner ppRNFL in albinism (i.e., thicker nasally and thinner temporally) support this supposition.

Peripapillary RNFL

We observed that ppRNFL in the outer annulus (i.e., 2.4–3.2-mm diameter), representing the number of nerve fibers entering the optic nerve, was strikingly thinner in the PWA group compared with controls, especially in temporal segments. Several studies suggest the possibility of reduced numbers of retinal neuronal populations in albinism. Akeo et al.[18] found reduced number of ganglion cells and an immature RNFL in a 19-week-old fetus with oculocutaneous albinism. Also magnetic resonance imaging studies have visualized smaller-sized postorbital optic nerves in albinism.[9,19] Also, abnormal distribution of the GCL as well as inner and the outer nuclear layers in the foveal region have been described both in the albino ferret[20] and in humans with albinism,[5,21] although it is not clear whether a reduction in cell numbers can be inferred or whether this indicates a redistribution of neuronal populations.

In contrast to thinner ppRNFL, we observed significantly larger rim volumes in albinism compared with controls. Histological studies report that the prelaminar aspect of the ONH comprises mainly retinal ganglion cell axons and glial cells.[22] During embryological development, both these cell populations shrink and the degree of regression determines the size of the optic cup and rim.[23,24] Consequently, smaller optic cups and larger rim volumes could indicate that this regression process is arrested in albinism, as suggested by Fulton et al.[25] Because there is evidence that ganglion cell numbers are reduced in albinism,[18] the larger rim volumes in albinism also could be due to excess glial tissue remaining from embryological development. Another possibility is that reorganization of retinal nerve fibers approaching the optic nerve leads to greater occupation of space. The degree of abnormality observed in PWA was consistent between right and left eyes, indicating that interrupted development impacts both eyes similarly.

Relationship Between ONH/ppRRNFL Abnormalities and Foveal Abnormalities

We observed a strong positive correlation between outer ppRNFL and GCL thickness at the central fovea ($P = 0.007$). In the normal central retina, the GCL is very thin due to centrifugal migration of inner retinal layers during development. One might expect an inverse correlation between outer ppRNFL and central GCL thickness, so that significant foveal hypoplasia is associated with ppRNFL thinning. The significant positive correlation could indicate that in albinism, GCL thickness at the central fovea represents GCL thickness across the retina. Consequently, ppRNFL thinning in albinism could reflect GCL thinning across the retina.

Relationship Between Disc/ppRRNFL Abnormalities and Clinical Measures

Several ONH abnormalities in albinism were negatively correlated with refractive errors, such as disc and cup areas. These could be due to the ONH changing in proportion with changes in eye axial length. One of the most consistent features of the ONH in albinism was horizontal elongation of

TABLE 1. Linear Regression Analysis Between ONH And ppRNFL Parameters And Central Foveal Measures

		Areas			Volumes		Ratios		ppRNFL Thickness	
Parameter	Statistic	Disc	Cup	Rim	Cup	Rim	Cup:Disc Ratio	H:V Disc Ratio	Inner Annulus	Outer Annulus
Macular thickness	*r*	−0.138	−0.221	0.019	−0.272	0.282	−0.200	−0.169	0.098	0.174
	P	0.372	0.149	0.905	0.074	0.064	0.193	0.273	0.543	0.290
Inner layers (ILM-OPL)	*r*	−0.153	−0.136	−0.055	−0.204	0.181	−0.086	−0.110	0.159	**0.320**
	P	0.322	0.377	0.724	0.184	0.239	0.577	0.479	0.322	**0.047**
Outer layers (ONL-BM)	*r*	0.088	−0.015	0.096	0.018	0.031	−0.063	−0.027	−0.093	−0.211
	P	0.572	0.922	0.535	0.906	0.842	0.686	0.863	0.562	0.198
Ganglion cell layer	*r*	−0.032	−0.091	0.032	−0.151	0.144	−0.090	−0.057	0.248	**0.427**
	P	0.838	0.559	0.837	0.328	0.352	0.561	0.711	0.118	**0.007**

Significant correlations are indicated in bold. H:V disc ratio, horizontal:vertical diameter disc ratio.

Table 2. Linear Regression Analysis Between ONH and ppRNFL Parameters and Clinical Measures

		Areas			Volumes		Ratios		ppRNFL Thickness	
Parameter	Statistic	Disc	Cup	Rim	Cup	Rim	Cup:Disc Ratio	H:V Disc Ratio	Inner Annulus	Outer Annulus
Refractive error (spherical equivalent)	*r*	**−0.435**	**−0.247**	−0.292	−0.205	0.019	**−0.213**	0.166	**0.182**	0.154
	p	**0.001**	**0.009**	0.129	0.051	0.458	**0.014**	0.150	**0.021**	0.455
Best-corrected visual acuity	*r*	**−0.383**	−0.174	−0.251	−0.209	−0.095	−0.116	0.015	−0.009	0.057
	p	**0.006**	0.223	0.075	0.140	0.508	0.420	0.919	0.950	0.708
Visual evoked potential asymmetry	*r*	−0.144	−0.211	0.008	−0.375	0.102	−0.219	−0.203	0.022	0.010
	p	0.503	0.323	0.970	0.071	0.636	0.303	0.340	0.924	0.966

Significant correlations are indicated in bold. H:V disc ratio, horizontal:vertical diameter disc ratio.

the disc. Interestingly, however, horizontal to vertical diameter disc ratio was not significantly correlated with refractive error, which suggests that this feature is not related to changes in the overall shape of the eye.

Surprisingly, best-corrected visual acuity was not correlated to the pattern of thinning of the temporal ppRNFL observed in albinism, an area typically containing the fibers of the papillomacular bundle. Also, although ppRNFL thickness in albinism was correlated with some measures of foveal hypoplasia, such as GCL thickness at the fovea, the correlation was mainly due to changes in the nasal rather than the temporal ppRNFL. This may indicate that the reduced numbers of fibers in the temporal ppRNFL observed in albinism (see Fig. 3) does not have a significant impact on fine spatial vision. In contrast, changes in foveal development in albinism, such as reduced cone elongation, have been demonstrated to be strongly correlated to visual acuity and are likely to be a key factor limiting fine spatial vision.[5]

In contrast to ppRNFL, best-corrected visual acuity was correlated to optic disc area with smaller disc sizes associated with worse visual acuity. It is difficult to know at this stage whether smaller disc sizes could directly lead to reduced visual acuity by limiting the establishment of connections between the eye and lateral geniculate nucleus during the development of the visual system. Alternatively, disc size could simply be a sensitive measure of the degree of albinism phenotype without being directly involved in influencing visual acuity. Further studies would help in establishing the most important determinants of vision in albinism, such as foveal and optic nerve abnormalities and nystagmus characteristics.

One limitation of this study was that genetic mutations had not been determined for the cohort, which can help in a definitive diagnosis of the type of albinism. However, using genetics to classify albinism also can be problematic because mutations cannot be located for a proportion of PWA. For example, a study by Hutton and Spritz[26] has found that mutations cannot be located for known OA genes for 24% of patients in a Caucasian population. Future studies to locate additional gene mutations along with a better understanding of genotype-phenotype correlations in albinism may help us to understand better the mechanisms behind optic nerve and foveal abnormalities.

Summary

Our study provides new information about the abnormal topography of the ONH in albinism and explains its appearance in the context of arrested development. Although treatment options for this disorder are currently limited, progress is under way to formulate suitable pharmacological and gene therapies to improve visual function in these patients.[27] This study provides an important reference point for assessing structural abnormalities of the ONH in albinism using OCT imaging.

Acknowledgments

Supported by the Medical Research Council (MR/J004189/1), Ulverscroft Foundation, and Medisearch Foundation. The authors alone are responsible for the writing and the content of the paper.

Disclosure: **S. Mohammad**, None; **I. Gottlob**, None; **V. Sheth**, None; **A. Pilat**, None; **H. Lee**, None; **E. Pollheimer**, None; **F.A. Proudlock**, None

References

1. Martinez-Garcia M, Montoliu L. Albinism in Europe. *J Dermatol*. 2013;40:319–324.
2. Sheth V, Gottlob I, Mohammad S, et al. Diagnostic potential of iris cross-sectional imaging in albinism using optical coherence tomography. *Ophthalmology*. 2013;120:2082–2090.
3. Sampath V, Bedell HE. Distribution of refractive errors in albinos and persons with idiopathic congenital nystagmus. *Optom Vis Sci*. 2002;79:292–299.
4. Wang J, Wyatt LM, Felius J, et al. Onset and progression of with-the-rule astigmatism in children with infantile nystagmus syndrome. *Invest Ophthalmol Vis Sci*. 2010;51:594–601.
5. Mohammad S, Gottlob I, Kumar A, et al. The functional significance of foveal abnormalities in albinism measured using spectral-domain optical coherence tomography. *Ophthalmology*. 2011;118:1645–1652.
6. Gimenez E, Lavado A, Jeffery G, Montoliu L. Regional abnormalities in retinal development are associated with local ocular hypopigmentation. *J Comp Neurol*. 2005;485:338–347.
7. Apkarian P, Reits D, Spekreijse H, Van Dorp D. A decisive electrophysiological test for human albinism. *Electroencephalogr Clin Neurophysiol*. 1983;55:513–531.
8. Spedick MJ, Beauchamp GR. Retinal vascular and optic nerve abnormalities in albinism. *J Pediatr Ophthalmol Strabismus*. 1986;23:58–63.
9. Schmitz B, Schaefer T, Krick CM, Reith W, Backens M, Kasmann-Kellner B. Configuration of the optic chiasm in humans with albinism as revealed by magnetic resonance imaging. *Invest Ophthalmol Vis Sci*. 2003;44:16–21.
10. Kaimbo DK. Tilted disc syndrome in Congolese patients. *J Fr Ophtalmol*. 2010;33:174–177.
11. Lee H, Sheth V, Bibi M, et al. Potential of handheld optical coherence tomography to determine cause of infantile nystagmus in children by using foveal morphology. *Ophthalmology*. 2013;120:2714–2724.
12. Chong GT, Farsiu S, Freedman SF, et al. Abnormal foveal morphology in ocular albinism imaged with spectral-domain optical coherence tomography. *Arch Ophthalmol*. 2009;127:37–44.

13. Kumar A, Gottlob I, McLean RJ, Thomas S, Thomas MG, Proudlock FA. Clinical and oculomotor characteristics of albinism compared to FRMD7 associated infantile nystagmus. *Invest Ophthalmol Vis Sci*. 2011;52:2306–2313.
14. von dem Hagen EA, Houston GC, Hoffmann MB, Morland AB. Pigmentation predicts the shift in the line of decussation in humans with albinism. *Eur J Neurosci*. 2007;25:503–511.
15. Shinohara K, Moriyama M, Shimada N, et al. Analyses of shape of eyes and structure of optic nerves in eyes with tilted disc syndrome by swept-source optical coherence tomography and three-dimensional magnetic resonance imaging. *Eye*. 2013;27:1233–1241.
16. Park KA, Park SE, Oh SY. Long-term changes in refractive error in children with myopic tilted optic disc compared to children without tilted optic disc. *Invest Ophthalmol Vis Sci*. 2013;54:7865–7870.
17. Thomas MG, Kumar A, Mohammad S, et al. Structural grading of foveal hypoplasia using spectral-domain optical coherence tomography a predictor of visual acuity? *Ophthalmology*. 2011;118:1653–1660.
18. Akeo K, Shirai S, Okisaka S, et al. Histology of fetal eyes with oculocutaneous albinism. *Arch Ophthalmol*. 1996;114:613–616.
19. Kasmann-Kellner B, Schafer T, Krick CM, Ruprecht KW, Reith W, Schmitz BL. Anatomical differences in optic nerve, chiasma and tractus opticus in human albinism as demonstrated by standardised clinical and MRI evaluation [in German]. *Klin Mobl Augenheilkd*. 2003;220:334–344.
20. Jeffery G, Kinsella B. Translaminar deficits in the retinae of albinos. *J Comp Neurol*. 1992;326:637–644.
21. McAllister JT, Dubis AM, Tait DM, et al. Arrested development: high-resolution imaging of foveal morphology in albinism. *Vision Res*. 2010;50:810–817.
22. Trivino A, Ramirez JM, Salazar JJ, Ramirez AI, Garcia-Sanchez J. Immunohistochemical study of human optic nerve head astroglia. *Vision Res*. 1996;36:2015–2028.
23. Tasman W, Jaeger EA. *The Wills Eye Hospital Atlas of Clinical Ophthalmology*. 2nd ed. Philadelphia: Lippincott Williams & Wilkins; 2001.
24. Walsh FB, Hoyt WF, Miller NR. *Walsh and Hoyt's Clinical Neuro-Ophthalmology: The Essentials*. 2nd ed. Philadelphia: Wolters Kluwer Health/Lippincott Williams & Wilkins; 2008.
25. Fulton AB, Albert DM, Craft JL. Human albinism. Light and electron microscopy study. *Arch Ophthalmol*. 1978;96:305–310.
26. Hutton SM, Spritz RA. A comprehensive genetic study of autosomal recessive ocular albinism in Caucasian patients. *Invest Ophthalmol Vis Sci*. 2008;49:868–872.
27. Summers CG, Connett JE, Holleschau AM, et al. Does levodopa improve vision in albinism? Results of a randomized, controlled clinical trial. *Clin Experiment Ophthalmol*. 2014;42:713–721.

Investigative Ophthalmology & Visual Science